

Cornering stiffness estimation based on vehicle lateral dynamics

C. Sierra , E. Tseng , A. Jain & H. Peng

To cite this article: C. Sierra , E. Tseng , A. Jain & H. Peng (2006) Cornering stiffness estimation based on vehicle lateral dynamics, Vehicle System Dynamics, 44:sup1, 24-38, DOI: [10.1080/00423110600867259](https://doi.org/10.1080/00423110600867259)

To link to this article: <https://doi.org/10.1080/00423110600867259>



Published online: 04 Apr 2007.



Submit your article to this journal [↗](#)



Article views: 3303



View related articles [↗](#)



Citing articles: 17 View citing articles [↗](#)

Cornering stiffness estimation based on vehicle lateral dynamics

C. SIERRA[†], E. TSENG[‡], A. JAIN[†] and H. PENG^{*†}

[†]Department of Mechanical Engineering, University of Michigan, Ann Arbor, Michigan, USA

[‡]Research/Advanced Engineering, Ford Motor Company

In this article, the cornering stiffness estimation problem based on the vehicle bicycle (one-track) model is studied. Both time-domain and frequency-domain-based methods are analyzed, aiming to estimate the effective cornering stiffness, defined as the ratio between the lateral force and the slip angle at the two axles. Several methods based on the bicycle model were developed, each having specific pros/cons related to practical implementations. The developed algorithms were evaluated on the basis of the simulation data from the bicycle model and the CarSimTM software. Finally, selected algorithms were evaluated using experimental data.

Keywords: Road friction estimation; Tire force; Lateral dynamics

1. Introduction

Tire/road friction is an important characteristic that influences vehicle longitudinal, lateral/yaw and roll motions. The tire/road friction coefficient, if accurately and timely obtained, could significantly impact the design and performance of active safety systems. This is because vehicle motions are predominantly affected through the tire forces, governed by road friction and tire normal forces. In the literature, the majority of tire–road friction estimation schemes use features of tire/tread behavior (*e.g.* wheel speed, wheel acceleration, aligning moment, tire noise) as the basis of the estimation. For example, Eichhorn and Roth [1] used optical and noise sensors at the front-end of the tire, and stress and strain sensors inside the tire's tread to study both parameter-based and effect-based road friction estimation methods. Ito *et al.* [2] used the applied traction force and the resulting wheel speed difference between driven and non-driven wheels to estimate the road surface condition. Pal *et al.* [3] applied the neural-network-based identification technique to predict the road frictional coefficient based on steady-state vehicle response signals. Pasterkamp [4] developed an on-line estimation method based on lateral force and self-aligning torque measurements and the Delft tyre model. Gustafsson [5] developed a model-based approach, and used the difference between driven and un-driven wheels to detect the tire–road friction. Liu and Peng [6] applied the special structure of the brush tire model and used the wheel speed signal to estimate the

*Corresponding author. Email: hpeng@umich.edu

road friction coefficient and cornering stiffness. These friction estimation methods identify tire/road characteristics by using longitudinal and tire dynamics, which can then be used for the adaptations of control/estimation algorithm for both lateral and longitudinal directions.

The goal of this article is to study **the possibility of using vehicle lateral/yaw dynamics for the estimation of road friction**, that is, based on the simple bicycle model (which is also known as the one-track model). The assumption is that estimation methods using vehicle motion data are fundamentally more robust when compared with those using tire behaviors. The reason is that **the tire has smaller inertia, and its behavior is influenced by road roughness**, anti-lock braking system (ABS) operation, tire pressure and tread variations, carcass radial non-uniformities and vehicle roll/pitch/vertical motions. Therefore, **tire motions tend to be a lot more oscillatory and contain higher frequency components**. Separating the effects of these disturbances from those of tire/road friction is difficult. Another benefit of **using lateral/yaw dynamics for cornering stiffness estimation** is that the related signals (such as steering angle, yaw rate, lateral acceleration and vehicle forward speed) are readily measured for other purposes. Therefore, incremental hardware cost is low.

Estimation methods based on vehicle lateral/yaw dynamic equations (mostly based on the bicycle model) can be divided into two categories: time-domain methods [7, 8] and transfer-function methods [9]. The time-domain methods use the dynamic equations either directly or in various combinational forms, and the underlying equations are correct even when the vehicle is time-varying, for example, due to the variation of vehicle longitudinal speed or road friction. On the other hand, the transfer-function representations of dynamic systems are accurate only when the vehicle is time-invariant, and the effects of transient dynamics are ignored. Therefore, transfer-function methods perform satisfactorily only under linear operating region where cornering stiffness remains constant. In reference [9], both the transfer-function based method and the variation-characteristic-speed-based method were presented. The latter can be said to be a special case of transfer-function methods, as it uses the zero-frequency (steady-cornering) information of the transfer function.

Despite of the benefits mentioned earlier, there are also **drawbacks of using lateral/yaw dynamics**. As the frequency content of relevant signals is lower, the obtained estimation may not be fast enough for certain applications, for example, ABS. In addition, vehicle lateral/yaw dynamics are inherently low-pass, and thus the estimation results are not as sensitive as tire-motion-based methods.

2. Vehicle model

The basis of our estimation methods is the bicycle (one-track) vehicle model, which describes the vehicle lateral and yaw dynamics of a 2-axle, 1-rigid body ground vehicle (figure 1). The state-space representation of this model is in the form

$$\begin{bmatrix} \dot{v} \\ \dot{r} \end{bmatrix} = \begin{bmatrix} \frac{-(C_{\alpha f} + C_{\alpha r})}{mu} & \frac{bC_{\alpha r} - aC_{\alpha f}}{mu} - u \\ \frac{bC_{\alpha r} - aC_{\alpha f}}{I_{zz}u} & \frac{-(a^2C_{\alpha f} + b^2C_{\alpha r})}{I_{zz}u} \end{bmatrix} \begin{bmatrix} v \\ r \end{bmatrix} + \begin{bmatrix} \frac{C_{\alpha f}}{m} \\ \frac{aC_{\alpha f}}{I_{zz}} \end{bmatrix} \delta_f \quad (1)$$

where u is the vehicle forward speed, v the vehicle lateral speed, r the yaw rate, m the vehicle mass, I_{zz} the yaw moment of inertia, $C_{\alpha f}$ and $C_{\alpha r}$ are the front and rear cornering stiffness (per axle), δ_f the front wheel steering angle, and a and b are the distances from the vehicle center of gravity to front and rear axles, respectively.

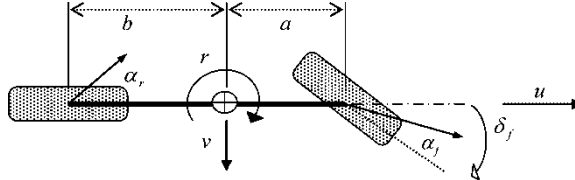


Figure 1. Two DOF (bicycle) model.

Equation (1) only includes steering input and ignores the effect of other inputs such as road-bank (super-elevation) angle. Therefore, the estimation will be obtained by observing the variation of state/output due to steering input perturbation. When road-bank angle exists, it is necessary to have an accurate road-bank estimation algorithm [10] in order to estimate cornering stiffness accurately. In this article, we will confine ourselves to scenarios where the road-bank angle is zero (except in the experimental evaluation). The cases with the road-bank estimator integrated can be extended, following the same problem format shown in ref. [11].

We also developed an enhanced version of the bicycle model which has non-linear tire look-up tables exported from CarSimTM. This enhanced bicycle model will be used to generate vehicle response used in the algorithm evaluation. The estimation algorithms will be evaluated on the basis of vehicle response data from three sources: the enhanced bicycle model, the CarSim [12] software and the experimental data provided by the Ford Motor Company [10, 11]. Figure 2 shows the comparison of vehicle response between the enhanced bicycle model and the CarSim model. It can be seen that the difference between these two models is small even when the lateral acceleration is as high as 0.6 g. This indicates that the bicycle model, with the non-linear tire look-up table, is a good approximation of the CarSim model.

An important difference between these two models was found to cause significant problems in the estimation – the phase lag between the tire slip angle and the tire lateral force. This lag

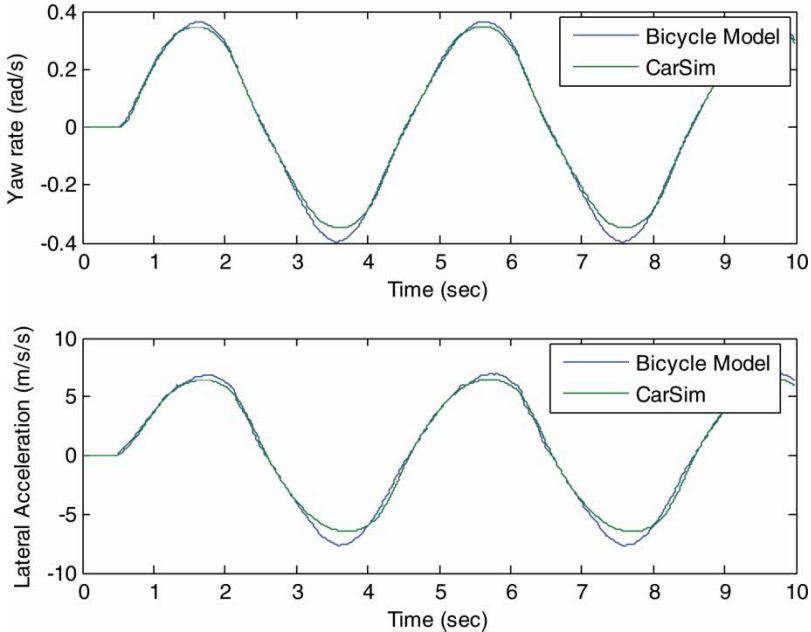


Figure 2. Response of bicycle model vs. CarSim.

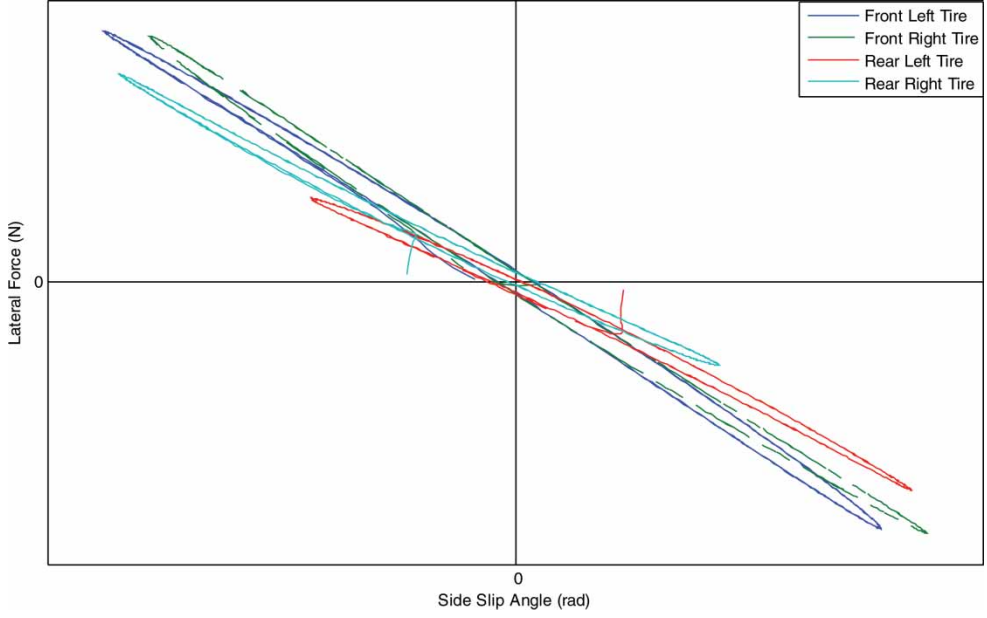


Figure 3. Tire force vs. tire slip angle (CarSim simulation results).

is likely the result of the tire relaxation length included in the CarSim software as well as the combination of the two (left and right) tire slip angles into one. The phase lag (shown in figure 3) makes it somewhat difficult to define the ‘true cornering stiffness’ from CarSim simulation results. As the stiffness to be estimated is the effective cornering stiffness, that is, the tire lateral force over tire slip angle, there is a singular point in generating the reference value when the tire slip angle passes through zero. Although the reference value differs from the constant cornering stiffness we are accustomed to, in a linear tire model, the effective cornering stiffness reflects the combined (left and right) lateral tire forces.

3. Direct method

This estimation method uses the two equations that form the state space of the bicycle vehicle model shown in equation (1). It is assumed that the vehicle parameters m , I_{zz} , a and b and the real-time measurements for δ_f , u , v and r are all available. We can use Euler’s approximation or other filtering schemes to approximate the derivative, \dot{r} (the lateral speed derivative). \dot{v} , if needed, is obtained in a different manner, as explained subsequently. Having all these variables, we can algebraically solve the two equations (equations (2) and (3)) for $C_{\alpha f}$ and $C_{\alpha r}$. The rearranged form of the solution, as per the definition of the (effective) cornering stiffness, is as follows

$$C_{\alpha f} = \frac{(b\dot{v}m + brmu + I_{zz}\dot{r})/L}{(-v - ra + \delta_f u)/u} = \frac{F_{yf}}{\alpha_f} \quad (2)$$

$$C_{\alpha r} = \frac{(armu + a\dot{v}m - I_{zz}\dot{r})/L}{(rb - v)/u} = \frac{F_{yr}}{\alpha_r} \quad (3)$$

It should be noted that even though, in equations (2) and (3), it appears we are using the derivative of the lateral velocity in the calculation, in the implementation, we actually use

$a_y - ur$ in place of \dot{v} , which is much easier to measure when compared with \dot{v} . It is important to note that for this estimation method, the values for the cornering stiffness, $C_{\alpha f}$ and $C_{\alpha r}$, could approach infinity when the slip angles, α_f and α_r , approach zero during a transient maneuver or when the vehicle is driving straight. Also, the slip angles could become large as the longitudinal speed u approaches zero. Given that these two singularity conditions create undesired estimation results, in the final implementation form, we will discard the estimation of the cornering stiffness outside of a defined set of threshold limits and stop the estimation scheme when the tire slip angle is small. In these cut-off cases, we will keep the last estimated values as our best guess. This modification is necessary to ensure that the overall estimation is reasonable. In addition, we will use signals within a horizon and use the least-square solution to generate the best fit for the overall horizon. The direct method is a straightforward two-unknown two-equation problem, and a reasonably good estimation is usually obtained.

As stated before, the ‘direct method’ is conceptually simple and straightforward. The problem is also numerically well-behaved. However, it requires both the lateral velocity (equivalently, side slip angle) and the derivative of the vehicle yaw rate – both of which are difficult to obtain reliably in real applications. We will investigate its performance with the estimated lateral velocity [11, 13], with simulation and experimental data. As this article is confined in the analysis without the road-bank angle, the lateral velocity estimator will assume no bank.

In the next several sections, we will present several variations of the direct method, each with its own benefits/drawbacks.

3.1 The ‘ a_y -method’

The basic idea of the so-called ‘ a_y -method’ is to eliminate reliance on the derivative of vehicle yaw rate. This can be achieved by using only the first equation (a_y) of the state-space equation

$$F_y = ma_y = C_{\alpha f}\alpha_f + C_{\alpha r}\alpha_r = C_{\alpha f}\left(\delta - \frac{v + ar}{u}\right) + C_{\alpha r}\left(-\frac{v - br}{u}\right) \quad (4)$$

which can be rewritten in standard regression form

$$\left[\delta - \frac{v + ar}{u} \quad -\frac{v - ar}{u}\right] \begin{bmatrix} C_{\alpha f} \\ C_{\alpha r} \end{bmatrix} = ma_y \quad (5)$$

Equation (5) can be formulated as a least-square estimation problem with one equation and two unknowns. When signals at multiple sampling instances are used, the problem can become over-determinate and the least-square solution can be obtained. The estimation method includes the following drawbacks: it still requires lateral velocity (side slip angle) and it is an under-determinate problem in nature and thus requires persistent excitation to obtain accurate results.

3.2 The ‘rdot-method’

One of the most important disturbance to equation (1) is the road-bank angle. The presence of gravity component in the lateral direction changes the lateral dynamics, and thus both the direct method (equation (1)) and the a_y -method (equation (5)) are susceptible to the presence of road-bank angle. If one relies on the second equation of equation (1), that is, the yaw acceleration equation (or the rdot equation), the resulting algorithm will be more robust with

respect to the road super-elevation disturbance. The fundamental equation is

$$M_{zz} = I_{zz}\dot{r} = aC_{\alpha f}\alpha_f - bC_{\alpha r}\alpha_r = aC_{\alpha f}\left(\delta - \frac{v + ar}{u}\right) - bC_{\alpha r}\left(-\frac{v - br}{u}\right) \quad (6)$$

which can be rewritten as

$$\left[a\left(\delta - \frac{v + ar}{u}\right) - b\left(-\frac{v - ar}{u}\right)\right]\begin{bmatrix} C_{\alpha f} \\ C_{\alpha r} \end{bmatrix} = I_{zz}\dot{r} \quad (7)$$

It can be seen that equation (7) relies on both lateral speed and yaw derivative. In addition, when the vehicle is cornering in steady state, the yaw acceleration is zero. Therefore, $[0; 0]$ would be a solution for equation (7). This observation predicts that the rdot-method, that is, the least-square estimation method based on equation (7), will not perform well when the vehicle is cornering at steady state. In addition, equation (7) is also under-determinate in nature and thus will work well only when persistent excitation condition is satisfied.

3.3 The ‘beta-less method’

All the three estimation methods require vehicle lateral velocity (or side slip angle), which is difficult to measure. In addition, the a_y -method and the rdot-method are both under-determinate. The method to be proposed here aims to address both issues. We first start from the lateral equation

$$ma_y = F_{yf} + F_{yr} = C_{\alpha f}\left(\delta_f - \beta - \frac{ar}{u}\right) + C_{\alpha r}\left(-\beta + \frac{br}{u}\right) \quad (8)$$

based on which the lateral velocity can be solved

$$\beta = \frac{1}{C_{\alpha f} + C_{\alpha r}}\left[C_{\alpha f}\left(\delta_f - \frac{ar}{u}\right) + C_{\alpha r}\left(\frac{br}{u}\right) - ma_y\right] \quad (9)$$

Plug in equation (9) into the yaw equation

$$I_{zz}\dot{r} = aF_{yf} - bF_{yr} = aC_{\alpha f}\left(\delta_f - \beta - \frac{ar}{u}\right) - bC_{\alpha r}\left(-\beta + \frac{br}{u}\right), \quad (10)$$

one obtains

$$\begin{bmatrix} mL a_y & L\left(\delta - \frac{Lr}{u}\right) \end{bmatrix} \begin{bmatrix} X_1 \\ X_2 \end{bmatrix} = I_{zz}\dot{r} + mba_y, \quad (11)$$

where

$$X_1 \equiv \frac{C_{\alpha f}}{C_{\alpha f} + C_{\alpha r}} \quad \text{and} \quad X_2 \equiv \frac{C_{\alpha f}C_{\alpha r}}{C_{\alpha f} + C_{\alpha r}}.$$

After the intermediate parameters X_1 and X_2 were found, the cornering stiffness can be calculated from

$$C_{\alpha r} = \frac{X_2}{X_1} \quad \text{and} \quad C_{\alpha f} = \frac{X_1}{1 - X_1}C_{\alpha r}. \quad (12)$$

It can be seen that the two intermediate variables determine the ratio and the magnitude of the two cornering stiffness, respectively. In the least-square estimation problem formulation, one could put different weightings to the two variables, for example, more weights on X_2 to promote magnitude convergence.

Table 1. Drawbacks of the four methods presented in section 3.

	Relies on \dot{r}	Relies on v	Under-determinate	Sensitive to road-bank angle
Direct method (equation (1))	Yes	Yes		Yes
a_y method (equation (5))		Yes	Yes	Yes
rdot method (equation (7))	Yes	Yes	Yes	
Beta-less method (equation (11))	Yes		Yes	Yes

The beta-less method can also be derived by relating the front and rear tire forces. Again starting from the lateral equation

$$\begin{aligned}
 ma_y &= F_{yf} + F_{yr} = C_{\alpha f}\alpha_f + C_{\alpha r}\alpha_r = XC_{\alpha r}\left(\alpha_r + \left(\delta - \frac{Lr}{u}\right)\right) + C_{\alpha r}\alpha_r \\
 &= (X + 1)F_{yr} + XC_{\alpha r}\left(\delta - \frac{Lr}{u}\right), \quad \text{where } X = C_{\alpha f}/C_{\alpha r},
 \end{aligned} \tag{13}$$

one obtains

$$\begin{bmatrix} F_{yr} & \left(\delta - \frac{Lr}{u}\right) \end{bmatrix} \begin{bmatrix} X \\ C_{\alpha f} \end{bmatrix} = F_{yf} \tag{14}$$

Note that equation (14) can be verified in the same manner as equation (11), where the lateral forces F_{yf} and F_{yr} are computed by using the measurements a_y and \dot{r} .

3.4 Discussion

None of the four methods presented in this section is perfect. They all have certain drawbacks, as shown in table 1. The ‘under-determinate’ issue refers to the fact the estimation problem has more unknowns than equations. Therefore, information from multiple sampling points needs to be used, and the information has to be persistently exciting for the estimation results to converge to the true values. The last column is shown in grey color because one of the authors had developed a robust algorithm for the road-bank angle estimation in an earlier publication [10]. So from our viewpoint, that problem is not a major issue.

It is worthwhile to mention that the ‘under-determinate’ problem of the three estimation methods shown in sections 3.1–3.3 can be eliminated by assuming that the ratio between the front and rear cornering stiffness is fixed (which has been used in ref. [9]). This way, the number of unknown variable is reduced to one, and most numerical problems and requirements (persistent excitation) will disappear. Under steady cornering, when an under-determinate method experiences difficulty, this addition assumption provides a reasonable way to ensure good estimation results. In the later part of this article, when the beta-less method is augmented with this assumption, we will refer to it as the ‘beta-less plus’ method.

4. Transfer-function method

This estimation method uses the transfer function from δ_f to r , obtained from the bicycle vehicle model previously described. Even though the method might work for the transfer function from δ_f to v as well, we use only the δ_f to r transfer function because measuring yaw rate is more feasible and accurate than lateral velocity. If we re-write the state-space equation

in a simpler form:

$$\begin{bmatrix} \dot{v} \\ \dot{r} \end{bmatrix} = \begin{bmatrix} a_1 & a_3 \\ a_2 & a_4 \end{bmatrix} \begin{bmatrix} v \\ r \end{bmatrix} + \begin{bmatrix} b_1 \\ b_2 \end{bmatrix} \delta_f, \quad (15)$$

then it is straightforward to write the transfer function from steering to yaw rate as

$$H_{\delta_f \rightarrow r}(s) = \frac{b_2 s + (a_2 b_1 - a_1 b_2)}{s^2 - (a_1 + a_4)s + (a_1 a_4 - a_2 a_3)} = \frac{n_1 s + n_2}{s^2 + d_1 s + d_2} \quad (16)$$

where

$$\begin{aligned} d_1 &= \frac{C_{\alpha f} + C_{\alpha r}}{mu} + \frac{a^2 C_{\alpha f} + b^2 C_{\alpha r}}{I_z u}, \\ d_2 &= \frac{(C_{\alpha f} + C_{\alpha r})(a^2 C_{\alpha f} + b^2 C_{\alpha r}) - (b C_{\alpha r} - a C_{\alpha f})[(b C_{\alpha r} - a C_{\alpha f}) - mu^2]}{m I_z u^2}, \\ n_1 &= \frac{a C_{\alpha f}}{I_z} \quad \text{and} \quad n_2 = \frac{L C_{\alpha f} C_{\alpha r}}{m I_z u}. \end{aligned}$$

This method uses the available parameters (m , I_z , a and b) and the measurements (δ_f , u and r) to obtain a least-square fit for the transfer function in real time. Ideally, in order not to rely on the derivative(s) of yaw rate, the estimation algorithm will be applied to the discrete-time format. In other words, the continuous-time transfer function shown in equation (16) should first be converted to its discrete-time counter-part, which can then be used to formulate an optimal estimation problem, for example, least-square ARX model identification problem. The identified ARX model, which best describes the vehicle yaw motion in the discrete-time format, will then be converted into the continuous-time where best-guess parameters of the transfer function for the yaw rate output [equation (16)] can be obtained. As the parameters of the continuous time transfer function are related to the cornering stiffness, it results in a non-linear set of four equations with two unknowns. We can solve this system using a least-square approach to obtain the best guess for the cornering stiffness.

5. Simulation results

In this section, the performance of the five methods are studied using the simulation data taken from the bicycle model with non-linear tires as well as the CarSim [12] software, for which model the input was the steering wheel angle. The estimation schemes, however, assume that the tire steering angle is directly measured. Therefore, the steering system dynamics included in the CarSim software will not have any adverse effect on our estimation results. In sections 5.1 and 5.2, we will examine the results of the four time-domain-based algorithms. In section 5.3, we will present the results from the transfer-function-based method.

5.1 Results based on the enhanced bicycle model data

We first examine the performance of the four time-domain estimation methods with the vehicle response data generated from the enhanced bicycle model. In this case, there is almost no uncertainty. The only uncertainty, from the viewpoint of the estimation methods, is the difference between the linear tire and the non-linear tire model. The results in this section serve to weed out the weakest algorithms so that future study will be more focussed. In addition, to fully demonstrate the performance of the algorithms in its cleanest form, we are not imposing any

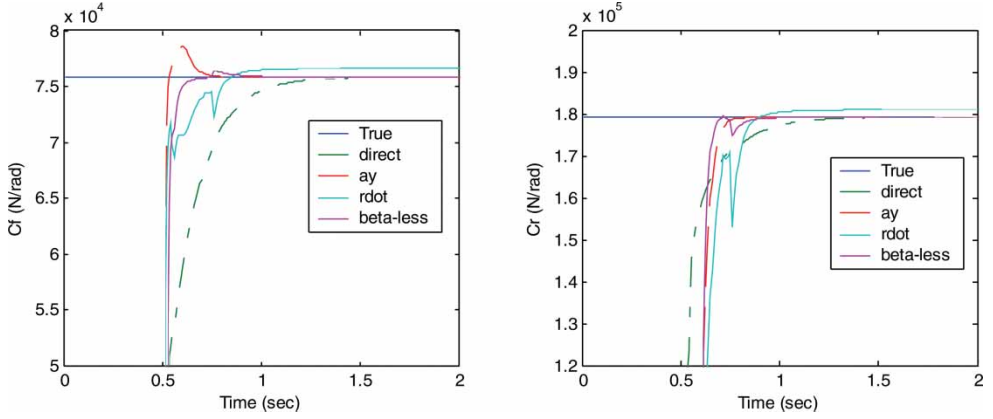


Figure 4. Estimation performance of the time-domain estimation methods (bicycle model data, J-turn).

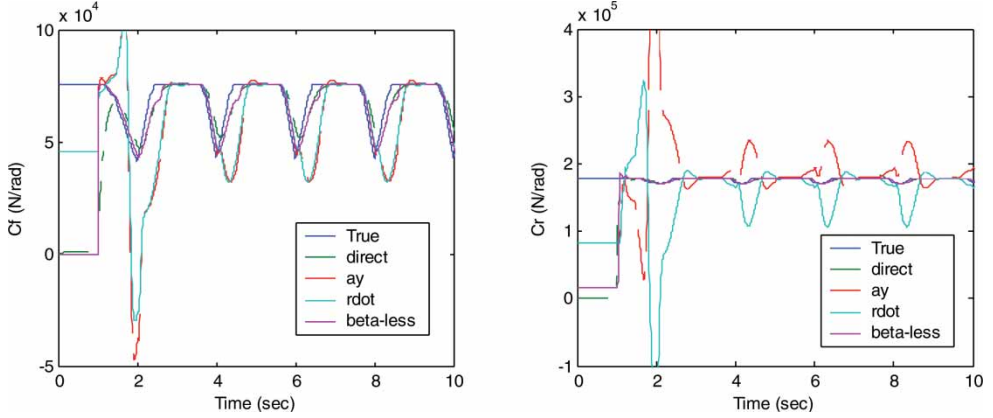


Figure 5. Estimation performance of the time-domain estimation methods (bicycle model data, slalom test).

filtering/saturation of the estimation results. For example, the estimated cornering stiffness values may become negative even though we know they should not. In all algorithms, the vehicle input and output data are obtained at the rate of 100 Hz, and 10 data points (over a 100 m s window) are used for the least-square estimations. Results from three maneuvers are presented: constant cornering (J-turn), slalom and fish hook. The results are shown in figures 4, 5 and 6, respectively.

It can be seen that the performance of the a_y -method and the r_{dot} method is significantly worse than the other two methods. For the direct method and the beta-less method, the performance is quite satisfactory. Other than during the initial phase, when the estimated variables converge gradually, both methods produce results that are very close to the true values all the time. In the following sections, we will focus on the direct method and the beta-less method for all future studies.

5.2 Results based on the CarSim data

In this section, the simulation data from the CarSim software is used. A major factor that needs to be considered is the availability of lateral velocity, which is difficult to measure in

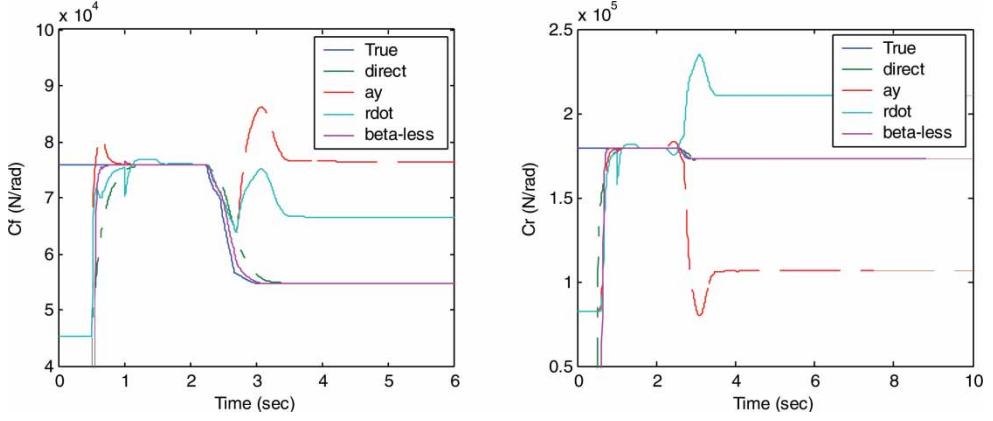


Figure 6. Estimation performance of the time-domain estimation methods (bicycle model data, fishhook).

the field. We will present results for two cases: when all needed signals are measured and when the lateral speed is estimated by using the algorithm presented in ref. [13]. Figures 7 and 8 show the results under two maneuvers: sinusoidal and fish hook. In each figure, we show the vehicle yaw rate and lateral velocity, which indicates the severity of the maneuver, and the estimation results. In the sinusoidal maneuver, the beta-less method performs better than the direct method – the latter exhibits some unwanted fluctuation due to zero crossing of the slip angle. When the estimated lateral velocity is used, the direct method performance is improved slightly.

In the fish hook maneuver, the direct method performs well, whereas the beta-less method does not. This is because the fish hook maneuver is not persistently exciting. Under this case, using the ‘plus-up trick’ (*i.e.*, assuming $C_{af}/C_{ar} = 1.2$) helps the beta-less method significantly. However, it can be seen that the transient performance suffers slightly. Therefore,

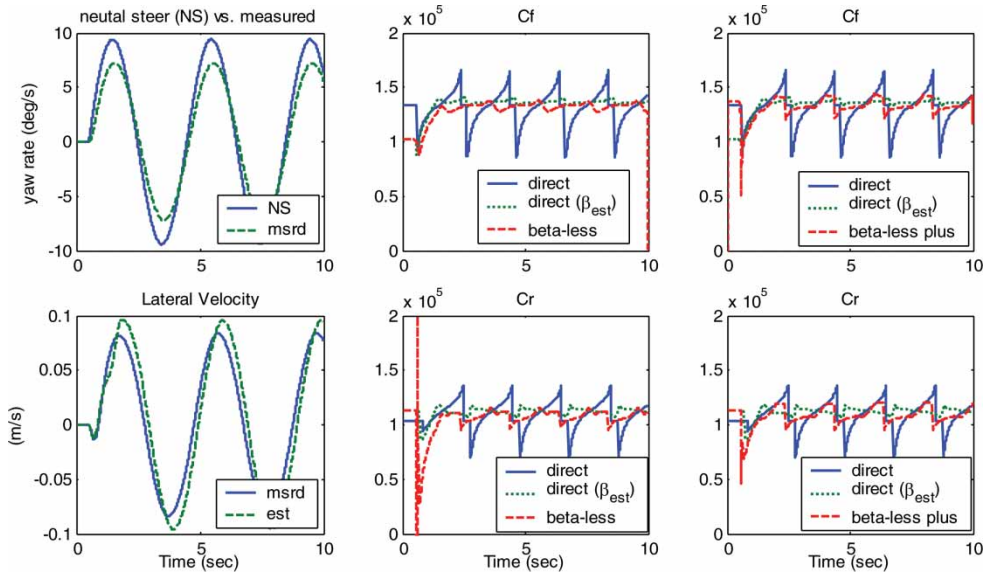


Figure 7. Estimation performance of the time-domain estimation methods (CarSim data, sinusoidal).

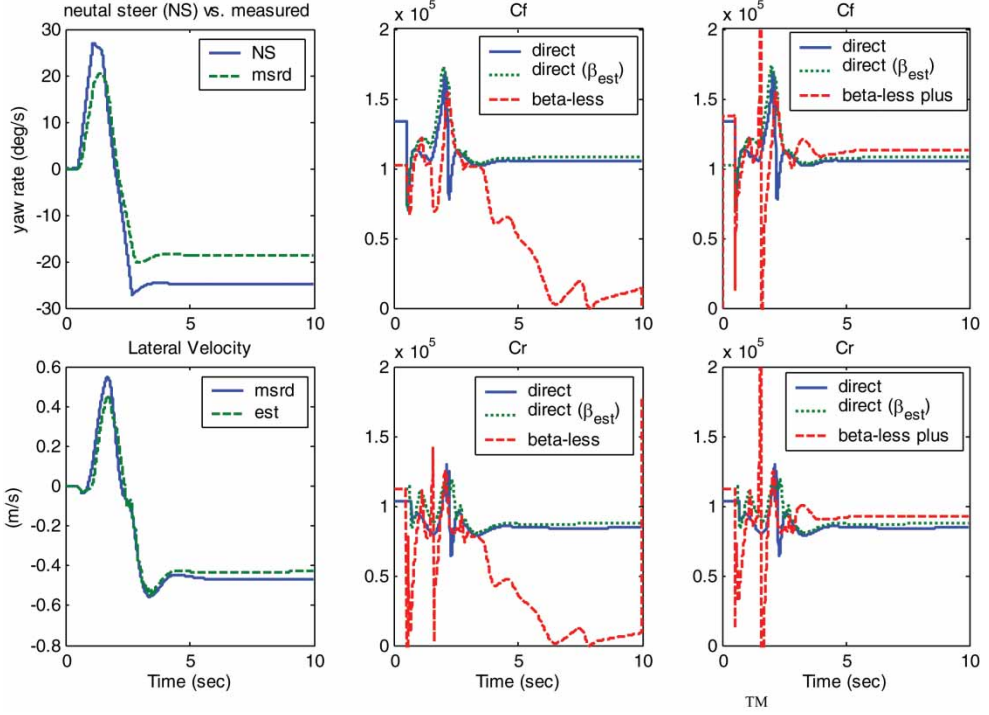


Figure 8. Estimation performance of the time-domain estimation methods (CarSim data, fish hook).

the original beta-less method should be used during transient, and switching to the beta-less plus method is beneficial only for steady-state conditions.

5.3 Results of the transfer-function method

On the surface, equation (16) is an over-determinate problem. When one uses least square, or any other methods to obtain ‘best-fit’ transfer function over a window, a transfer function with four known coefficients (n_1 , n_2 , d_1 and d_2) will be obtained. These four coefficients are then used to obtain the best estimate for C_{af} and C_{ar} . As at each sampling time, there are four equations and two unknowns, we seem to have an over-determined problem. Therefore, persistent excitation is expected to be less of a problem. This observation turns out to be false, as will be shown in the following. In fact, we found the transfer-function estimation to be harder than many time-domain-based problems. We first start from an implementation of the transfer-function method that does not require derivatives, that is,

$$r(t) = -d_1 \int_0^t r(\tau) d\tau - d_2 \iint r(\tau) d\tau + n_1 \int_0^t \delta(\tau) d\tau + n_2 \iint \delta(\tau) d\tau + c_1 t + c_2. \quad (17)$$

We then solve the least-square problem to identify these six unknown coefficients [for the six terms of equation (17)]. The cornering stiffness C_{af} and C_{ar} are then obtained. Figure 9 shows that the estimated values are way-off but the estimated yaw rate tracks the true yaw rate value exactly. In other words, we seem to have an under-determinate problem. To study this issue further, we ran the least-square estimation problem with three different initialization schemes: (i) starting from a constant value of $C_{af0}(k) = C_{ar0}(k) = 1e4$; (ii) $C_{af0}(k) = C_{af}(k-1)$,

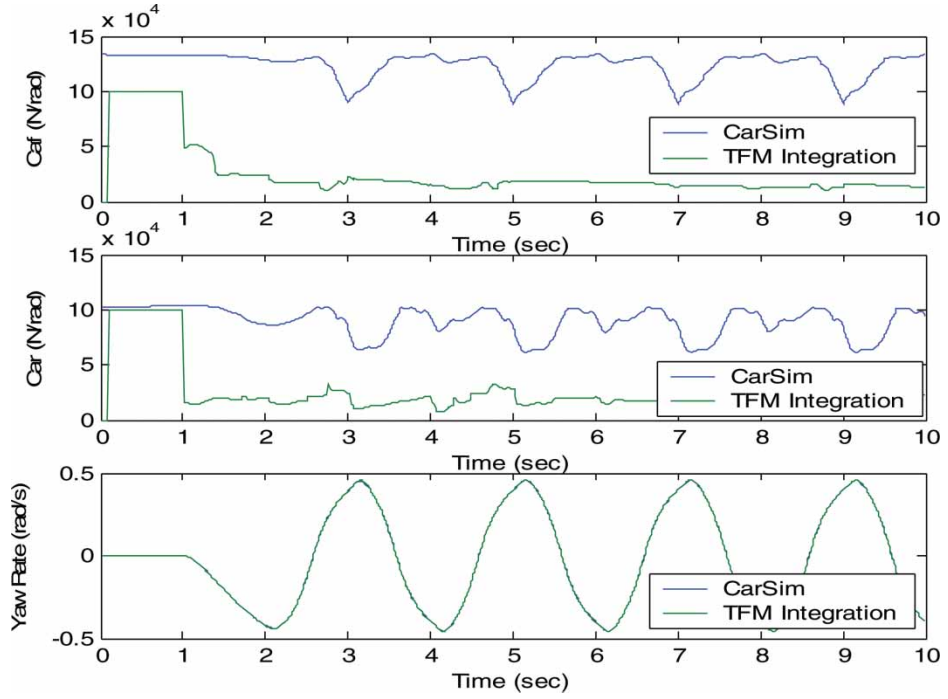


Figure 9. Estimation performance of the transfer-function (integration) method (CarSim data, sinusoidal).

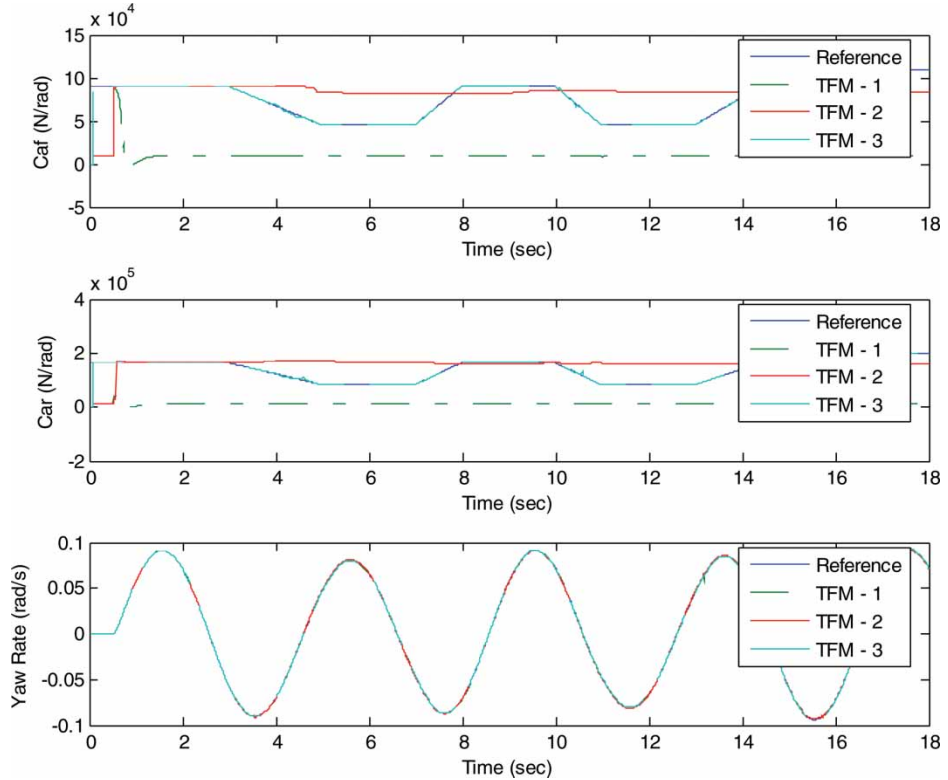


Figure 10. Estimation performance of the transfer-function method (bicycle mode data, sinusoidal).

$C_{\alpha r0}(k) = C_{\alpha r}(k - 1)$; (iii) $C_{\alpha f0}(k) = C_{\alpha f_true}$, $C_{\alpha r0}(k) = C_{\alpha r_true}$. These three estimation methods, referred as TFM1, TFM2 and TFM3, will be tested under an imaginary case when the (original) bicycle model cornering stiffness is varying slowly. The estimation results are shown in figure 10. All the three methods result in perfectly reconstructed yaw rate. However, the cornering stiffness values are quite different—in other words, we have an under-determinate problem. This fact makes it extremely difficult to obtain accurate cornering stiffness using the transfer-function method. Using the original equation (16) (using derivatives of signals) reduces the number of unknowns to 4, but the results are still unsatisfactory. We had also tried a discrete-time implementation, but the results were similar.

6. Experimental results

In this section, the performance of the direct method and the beta-less methods is studied using test data from a Lincoln Mark 8 vehicle, obtained at the Smithers Winter Test Center (low friction) and Ford Michigan Proving Ground (high friction) [10, 11]. The steering inputs and the vehicle speed were controlled by a human driver and vary in an arbitrary fashion. All vehicle lateral dynamical variables are directly measured, except lateral speed, which may be measured or estimated [13]. All the test data were measured at the sampling time of 7 m s.

Two challenging test conditions were selected: slalom on a high- μ and banked road surface and wobbly on icy surface. In the first case (figure 11), the lateral speed estimation has an

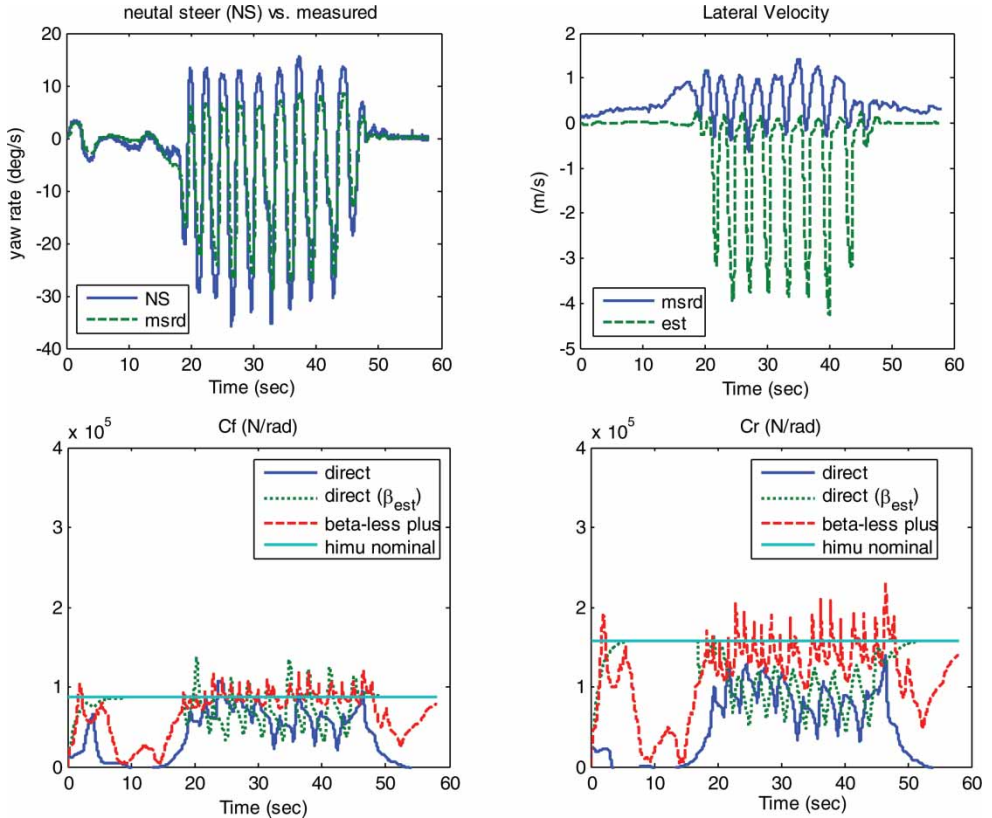


Figure 11. Estimation performance of the direct and beta-less methods (test data, high- μ on bank).

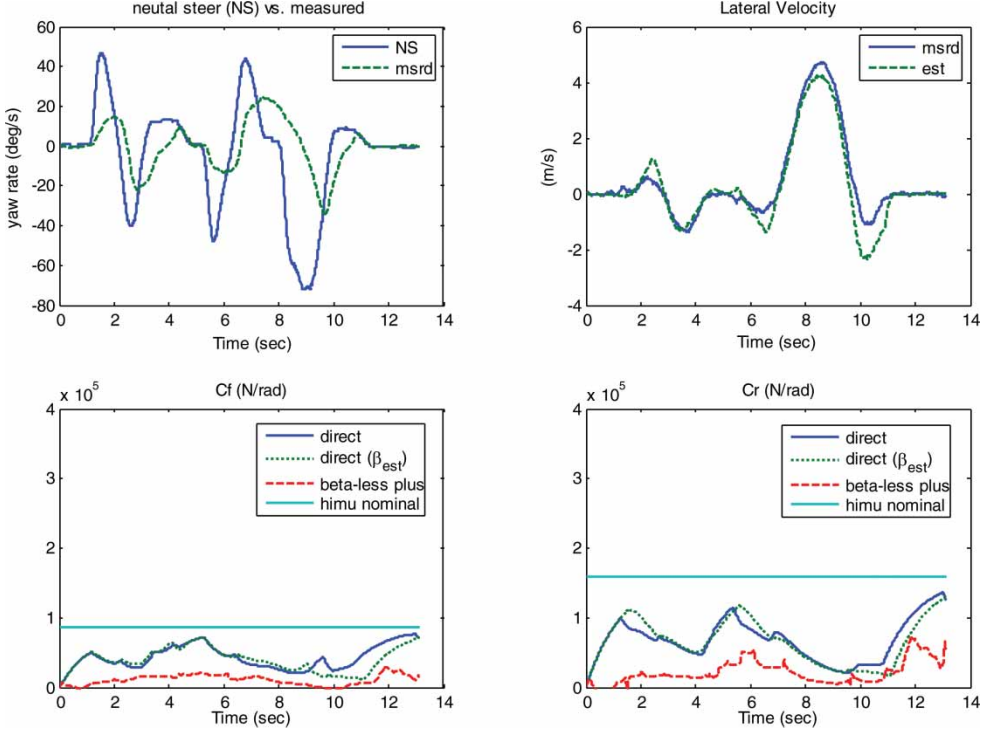


Figure 12. Estimation performance of the direct and beta-less methods (test data, low- μ flat road).

obvious offset. Both versions of the direct methods return estimated values that are slightly below the true value. The beta-less plus method, on the contrary, returns reasonable results. It should be noted that in this severe slalom maneuver, the true effective cornering stiffness should fluctuate somewhat similar to the case shown in figure 5. In the test, as we do not have a real-time measurement of tire cornering stiffness, we are only showing the nominal high- μ value which indicates where the true value should be roughly located.

In the icy-road scenario (figure 12), again there is no way we can measure the true values of the cornering stiffness. The true value is lower than the ‘high- μ nominal’ line shown in the plots, but we do not know exactly where. The estimated results of the two methods are quite different, and we cannot tell for certain which method is more accurate. More experimental work needs to be done, which the authors are inspired to work on.

7. Conclusions

In this article, we studied the application of vehicle lateral dynamic equations to the estimation of tire cornering stiffness. The estimation methods are based on the simple bicycle model and common lateral/yaw measurement. It was found that the under-determinateness is a major issue and should be avoided if possible. Among all the methods studied, the direct method and the beta-less method were found to have the highest potential for field implementation. Preliminary study using pre-recorded experimental data shows that they work reasonably well under two highly challenging experimental scenarios.

References

- [1] Eichhorn, U. and Roth, J., 1992, Prediction and monitoring of tyre/road friction, Proceedings FISITA, London, June.
- [2] Ito, M., Yoshioka, K. and Saji, T., 1994, Estimation of road surface conditions using wheel speed behavior. SAE paper no. 9438826.
- [3] Pal, C., Hagiwara, I., Morishita, S. and Inoue, H., 1994, Application of neural networks in real time identification of dynamic structural response and prediction of road-friction coefficient from steady state automobile response. SAE paper no. 9438817.
- [4] Pasterkamp, W.R., 1997, *The Tyre as Sensor to Estimate Friction* (Delft, The Netherlands: Delft University Press).
- [5] Gustafsson, F., 1998, Monitoring tire–road friction using the wheel slip. *IEEE Control Systems Magazine*, **18**, 42–49.
- [6] Liu, C. and Peng, H., 1996, Road friction coefficient estimation for vehicle path prediction. *Vehicle System Dynamics*, **25**(Suppl.), 413–425.
- [7] Han, J., Rajamani, R. and Alexander, L., 2002, GPS-based real-time identification of tire–road friction coefficient. *IEEE Transaction on Control System Technology*, **10**(3), 331–343.
- [8] Arndt, M., Ding, E.L. and Massel, T., 2004, Identification of cornering stiffness during lane change maneuvers. Proceedings of the 2004 International Conference on Control Applications, Taipei, Taiwan, pp. 344–349.
- [9] Börner, M. and Isermann, R., 2004, Adaptive one-track model for critical lateral driving situations. Proceedings of the 6th International Symposium on Advanced Vehicle Control (AVEC), Hiroshima, Japan.
- [10] Tseng, H.E., 2001, Dynamic estimation of road bank angle. *Vehicle System Dynamics*, **36**(4–5), 307–328.
- [11] Ungoren, A.Y., Peng, H. and Tseng, H., 2004, A Study on lateral speed estimation methods. *International Journal of Vehicle Autonomous Systems*, **2**(1/2), 126–144.
- [12] Mechanical Simulation Corporation, Ann Arbor, MI 48103, <http://www.carsim.com/>
- [13] Tseng, H.E., 2002, A sliding mode lateral velocity observer. Proceedings of the 6th International Symposium on Advanced Vehicle Control (AVEC), Hiroshima, Japan.